Int. J. Electron. Commun. (AEÜ) 86 (2018) 133–141

Contents lists available at ScienceDirect

Int. J. Electron. Commun. (AEÜ)

journal homepage: www.elsevier.com/locate/aeue

Regular paper

An offset CPW-fed triple-band circularly polarized printed antenna for multiband wireless applications

Ashok Kumar[a,*], Venuka Sankhla[a], Jitendra Kumar Deegwal[b], Arjun Kumar[c]

[a] Department of Electronics and Communication Engineering, Government Mahila Engineering College, Ajmer, India
[b] Department of Electronics Instrumentation & Control Engineering, Government Engineering College, Ajmer, India
[c] School of Engineering and Applied Sciences, Bennett University, Greater Noida, India

ARTICLE INFO

Keywords:
Circular polarization
E-shaped patch
Printed antenna
Wireless communication frequencies

ABSTRACT

An offset coplanar waveguide (CPW)-fed triple-band circularly polarized tilted asymmetrical E-shaped printed antenna for multiband wireless applications is presented in this paper. The antenna mainly consists of a tilted asymmetrical E-shaped patch and excite by a 50 Ω offset CPW feed line using a transformer for impedance matching to generate wide quad operating bands. By properly embedding rectangular slots in the tilted asymmetrical E-shaped patch and triangular stubs loaded modified CPW ground plane, the antenna reveals triple-band circular polarization (CP) features. Numerical analysis and experimental validation of the antenna structure have been carried out and results are presented. The mechanism of triple-band CP operation, analysis of surface current distributions, design procedure, and parametric study of the design is discussed in details. It is well suited for the application of UMTS-2100, 3.5/5.5 GHz WiMAX, 5.2/5.8 GHz WLAN, ITS, downlink of X-band satellite communication, and ITU 8 GHz bands.

1. Introduction

Due to rapid growth in wireless technologies, circularly polarized (CP)/linearly polarized (LP) printed antennas have been found wide use and popular in modern mobile/wireless/satellite systems such as universal mobile telecommunication services (UMTS), wireless local area networks (WLAN), worldwide interoperability for microwave access (WiMAX), intelligent transport systems (ITS), international telecommunication union (ITU), and downlink of X-band satellite communication application due to certain advantages such as suppression in polarization mismatch, reduction in propagation loss and multipath effects with avert the issue of displacement. For that reason, a single antenna with multiband CP functionality has fascinated much attention for academician and researchers for covering almost the stated bands. To accomplish this some extent, the various kinds of CP/LP printed antennas have been studied and reported by using various methods and techniques to achieve linear and single/dual/multiband circular polarization. For satellite and terrestrial applications, a Y-shaped monopole antenna with omnidirectional radiation pattern, similar features of wire turnstile antenna is presented [1]. For wireless and satellite systems, a wideband CP slot antenna excited by modified L-shaped element [2], a slit in C-shaped radiator and embedded two triangular stubs in ground plane monopole antenna [3], a trapezoidal shape tuning stub slot antenna loaded with circular stubs in slot [4], a monofilar spiral stubs and a slit in asymmetrical ground plane loaded wideband printed antenna [5], and a wide slot with modified shape CPW-fed antenna [6] are demonstrated for single wide/broadband impedance bandwidth (IBW) and axial ratio bandwidth (ARBW) operation. A compact annular ring shaped antenna with an L-shaped slot and defected ground with C-shaped slot [7], a multistubs loaded resonator rectangular monopole antenna [8], a dual-polarized monopole antenna loaded with Ω-shaped slot and asymmetric U-shaped slot [9], a multi-polarized quad-band planar antenna loaded with parasitic double T-stub, long and short inverted L-stubs [10], asymmetric slits loaded irregular shaped microstrip patch antenna with defected ground structure [11] are reported for multiband wireless systems. A dual-band capacitively loaded annular-ring slot dual-sense CP antenna [12], a bevel rectangular and loaded I-shaped stub dual-band CP monopole antennas with embedded stepwise inverted-L slit and I-shaped stub in ground plane [13], a two-port wideband square slot antenna with asymmetric H-shaped feed lines and a T-shaped grounded stub for dual-band dual-sense CP operation [14], an electromagnetically coupled triple-band microstrip patch antenna with two substrate layers [15], an inverted rotated U-shaped radiator with embedded I-shaped and inverted-L-shaped strip

* Corresponding author.
E-mail addresses: kumarashoksaini@gmail.com (A. Kumar), venuka.sankhla2712@gmail.com (V. Sankhla), jitendradeegwal@gmail.com (J.K. Deegwal), akdec.iitr@gmail.com (A. Kumar).

https://doi.org/10.1016/j.aeue.2018.02.002
Received 2 October 2017; Accepted 2 February 2018

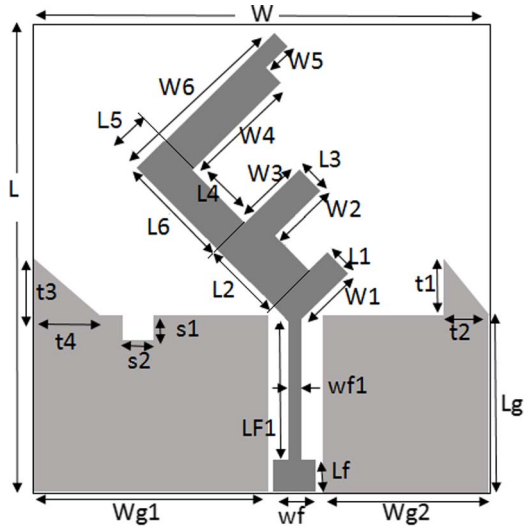

Fig. 1. Configuration of the proposed tilted asymmetrical E-shaped printed antenna.

Table 1
Parameters of the proposed antenna.

Parameter	*W*	*W1*	*W2*	*W3*	*W4*	*W5*	*W6*	*Wg1*	*Wg2*
Unit (mm)	50	10.58	9.19	10.96	17.25	2.47	25.46	25.65	20.65
Parameter	*Wf*	*Wf1*	*L*	*L1*	*L2*	*L3*	*L4*	*L5*	*L6*
Unit (mm)	3	1.5	58	3.62	10.42	4.27	10.8	5.74	15.4
Parameter	*Lf*	*Lf1*	*Lg*	*t1*	*t2*	*t3*	*t4*	*s1*	*s2*
Unit (mm)	3	16.15	19	7	6	7.5	7.5	4	5

printed dual-band antenna [16], a hexagonal slot antenna with multiple L-shaped slit arms [17], a rotated square patch antenna with embedded X-shaped, inverted-L shaped slit and two isosceles triangular stubs in ground plane with wide IBW [18] and a triple-band Y-shaped monopole antenna with L-shaped slot in ground plane [19] are proposed for triple-band circular polarization.

In this paper, an offset CPW-fed tilted asymmetrical E-shaped printed antenna is presented for multiband wireless applications. By embedding rectangular slots in the tilted asymmetrical E–shaped patch and triangular stubs loaded modified CPW ground plane, the triple–-band 3-dB ARBW and wide quad – 10 dB IBW could be obtained. The reflection coefficient ($|S_{11}|$) and axial ratio (AR) of each case is compared to show the effect on the antenna behavior by step wise design along with surface current distribution at three CP resonant frequencies, design procedure and parametric study of various dimensions are also discussed. The antenna structure has been fabricated, tested and experimentally studied.

2. Antenna design and analysis

2.1. Antenna configuration

The schematic configuration of the proposed offset CPW-fed tilted asymmetrical E-shaped printed antenna is shown in Fig. 1. The antenna is designed on low cost FR-4 glass epoxy dielectric substrate material having $\varepsilon_r = 4.3$, thickness of 1.6 mm, and loss tangent $\tan\delta = 0.025$. The antenna structure consists of a tilted asymmetrical E-shaped patch, triangular shaped stubs embedded modified CPW ground plane, and rectangular slots. The antenna is fed by 50 Ω offset CPW line with a width of w_f and length of L_f with an impedance transformer width w_{f1} and length L_{f1}. An offset in the CPW feed, asymmetric CPW ground planes with two triangular stubs and rectangular slot of size $s_1 \times s_2$ can develop the CP performance. Moreover, a rectangular slot is embedded on the upper arm of tilted asymmetrical E-shaped patch to improve the CP performance. The overall size of the proposed antenna is $50 \times 58\ mm^2$. The optimized parameters of the proposed offset CPW-fed tilted asymmetrical E-shaped printed antenna after numerically studied on CST Microwave Studio are listed in Table 1.

2.2. Design procedure

To investigate the antenna design, evolution stages of antenna is shown in Fig. 2. Initially, an offset CPW-fed tilted asymmetrical U-shaped printed antenna is designed as shown in Ant. 1 of Fig. 2. It provides three operating bands and resonating at around 3.4/5.35/7.15/8.4 GHz frequencies, but has poor axial ratio feature at around 5.5 GHz and 8.2 GHz. The tilted L-shaped stub is integrated in Ant. 1 as shown in Ant. 2 of Fig. 2 and structure becomes a tilted asymmetrical E-shaped printed antenna. Ant. 2 improves impedance matching and creates additional resonance at 2.1 GHz. In addition, the impedance bandwidth of the third band is improved and gives wideband behavior. Moreover, with the introduction of an offset in the feed and considering tilted asymmetrical E-shaped patch (Ant. 2 in Fig. 2), it is possible to establish current on the structure having two orthogonal field components at different frequencies. So, Ant. 2 shows poor axial ratio feature at three CP frequencies around 2.8/5.95/7.75 GHz but 2.8 GHz axial ratio does not match with the operating band. Therefore, two triangular shaped stubs are embedded in the CPW ground plane of Ant. 2 as shown in Ant. 3 of Fig. 2 to improve 2.8 GHz and 5.95 GHz axial ratio. It has similar reflection coefficient behavior of Ant. 2 but improves AR frequency due to identical horizontal and vertical surface currents generated on rectangular stubs. To further improves the CP performance, one rectangular slot embedded on the tilted asymmetrical E-shaped patch and another slot on the modified CPW ground plane as shown in Ant. 4 of Fig. 2. The triple CP bands at about 3.3 GHz, 5.05 GHz, and 7.3 GHz frequencies are obtained and slightly reflection coefficient changes. The triple CP bands may be due to having almost equal amplitude of horizontal and vertical surface currents among respective elements and 90° phase difference (PD). The CP and impedance matching performance is affected by varying the dimensions of

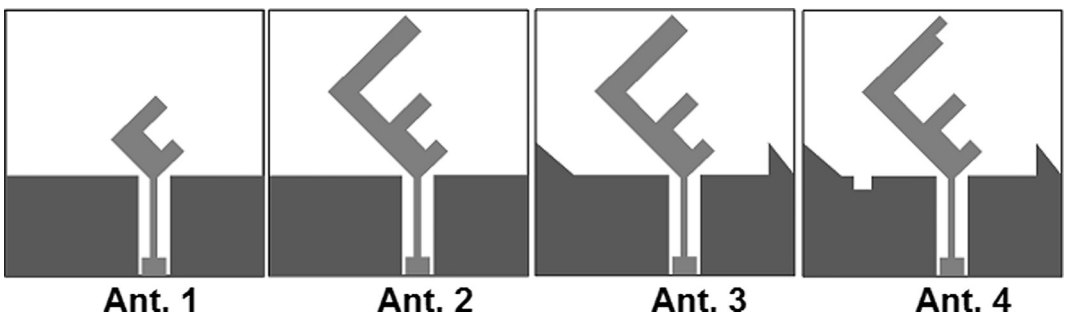

Fig. 2. Evolution of the proposed tilted asymmetrical E-shaped printed antenna.

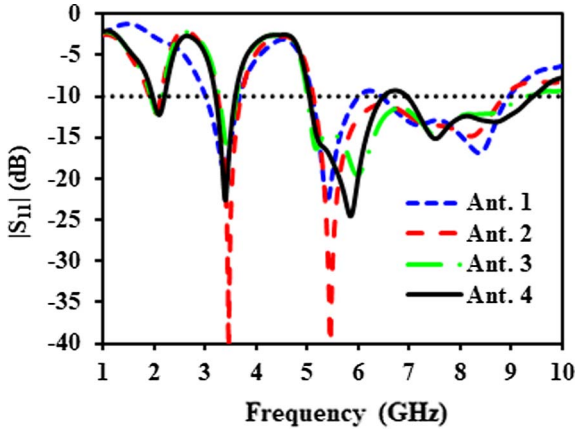

Fig. 3. $|S_{11}|$ comparison for different configurations of Fig. 2.

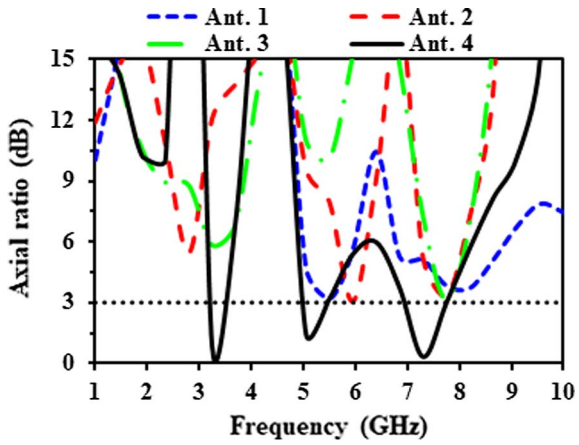

Fig. 4. Axial ratio comparison for different configurations of Fig. 2.

rectangular slots and offset in feed. From the design procedure, it may be concluded that by introduction of two triangular shaped stubs and rectangular slots along with proper adjusting offset can radiates triple-band CP waves. The comparison of reflection coefficient ($|S_{11}|$) and AR against frequency for different configurations of Fig. 2 are shown in Figs. 3 and 4, respectively. The detailed study of the evaluation stages in terms of $|S_{11}|$ and AR are summarized in Table 2.

2.3. Surface current distributions

To clarify the mechanism of radiation characteristics, the surface current distributions of Ant. 4 (proposed antenna) at four resonant frequencies 2.10, 3.40, 5.85, and 7.51 GHz have been illustrated in Fig. 5(a) to (d), respectively. From Fig. 5(a), it can be observed that mainly current concentrated on upper arm of tilted asymmetrical E-shaped patch (i.e., integrated L-shaped stub in Ant. 1) which creates resonance around 2.1 GHz. The resonance at about 3.4 GHz and 5.85 GHz is created due to mainly current concentrated on middle arm and lower arm of tilted asymmetrical E-shaped patch as shown in Fig. 5(b) and (c), respectively. The resonance at about 7.51 GHz may be created due to offset CPW-fed monopole antenna as current distribution shown in Fig. 5(d).

In order to analyze the CP mechanism of the proposed antenna, the surface current distributions at 3.3, 5.05, and 7.3 GHz at different time instants 0°, 90°, 180°, and 270° is depicted in Fig. 6. It can be observed that CP radiation at about 3.3 GHz is generated due to identical amplitudes and 90° PD on tilted E-shaped patch and rectangular slot in the modified CPW ground plane. Similarly, the CP radiation at about

Table 2
Comparisons of −10 dB $|S_{11}|$ impedance and 3-dB axial ratio bandwidths variations of the proposed antenna design procedure.

Antenna configuration	Antenna type	IBWs (GHz) ($\|S_{11}\| \le -10$ dB)	3-dB ARBWs (GHz)	Antenna response
Ant. 1	Tilted asymmetrical U-shaped patch	3.03–3.69 5.09–5.97 6.52–9.02	–	Triple-band
Ant. 2	Tilted asymmetrical E-shaped patch	1.90–2.13 3.25–3.70 5.12–8.87	–	Triple-band
Ant. 3	Tilted asymmetrical E-shaped patch with two triangular stubs	1.94–2.15 3.27–3.61 5.00–9.30	–	Triple-band
Ant. 4 (Proposed antenna)	Tilted asymmetrical E-shaped patch with two triangular stubs and rectangular slots	1.97–2.21 3.20–3.60 5.0–6.50 6.94–9.44	– 3.20–3.50 5.00–5.45 6.94–7.75	Quad-band

5.05 GHz and 7.3 GHz is due to middle and lower arm of tilted asymmetrical E-shaped monopole, embedded triangular stubs and etched rectangular slot in the modified CPW ground plane. From Fig. 6(a), it can be observed that at different time instants from 0° to 270° the resultant current vector rotates clockwise direction leads to contribute left-handed circular polarization (LHCP) radiation in direction of θ = 0°. As it can be seen from Fig. 6(b) and (c), it is observed that the resultant current vector rotates anticlockwise direction leads to contribute right-handed circular polarization in direction of θ = 0°. As a result, it may be concluded that at 3.3 GHz, the antenna radiates LHCP wave while at 5.05 GHz and 7.3 GHz, it radiates RHCP waves.

2.4. Mathematical formulation

The mathematical formulation can be understood through the current distribution of the proposed antenna as discussed in Section 2.3. It can be seen that at 2.1/3.4 GHz and 5.85 GHz frequencies, a large surface current is concentrated on the upper/middle (tilted horizontal and vertical) arms and lower arm of tilted asymmetrical E-shaped patch, respectively. This indicates that each of them acts as a half-wavelength resonator to generate first/second/third resonance modes and respective operating bands. The expression for the each half-wavelength resonator length can be calculated by (1)–(3) with the help of following formulas:

$$L_{r1} = L_6 + W_6 \tag{1}$$

$$L_{r2} = L_2 + L_5 + W_3 \tag{2}$$

$$L_{r3} = L_1 + W_1 + W_{f1} \tag{3}$$

The resonance frequency f_{ri} for ith half-wavelength resonator and effective dielectric constant (ϵ_{eff}) can be calculated using (4) and (5) as

$$f_{ri} = \frac{c}{2L_{ri}\sqrt{\epsilon_{eff}}}, \quad i = 1,2,3 \tag{4}$$

$$\epsilon_{eff} = \frac{\epsilon_r + 1}{2} \tag{5}$$

where c = velocity of light in free space (3×10^8 m/s). The calculated value of $\epsilon_{eff} = 2.65$.

From Table 1 for $i = 1$, $L_{r1} = 40.86$ mm and the calculated value of first resonance frequency $f_{r1} = 2.25$ GHz. Similarly, from Table 1 for $i = 2$, $L_{r2} = 27.12$ mm and the calculated value of second resonance frequency $f_{r2} = 3.39$ GHz. Also, from Table 1 for $i = 3$, $L_{r3} = 15.7$ mm

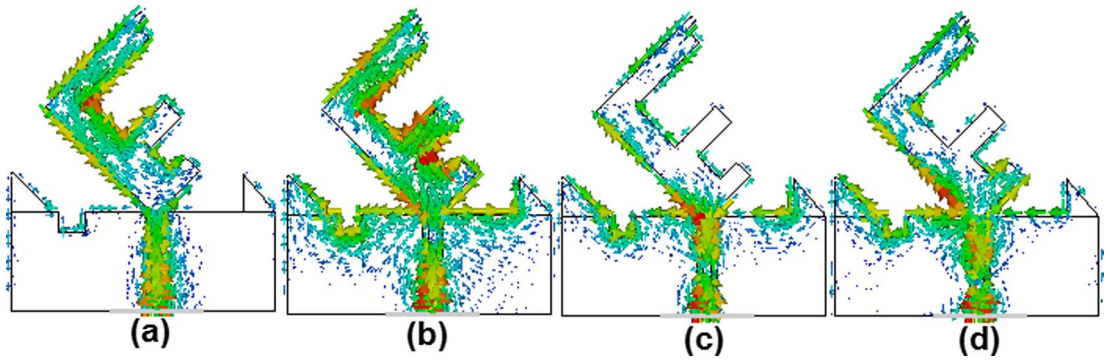

Fig. 5. Surface current distribution of the proposed tilted asymmetrical E-shaped printed antenna at (a) 2.1 GHz, (b) 3.40 GHz, (c) 5.85 GHz, and (d) 7.51 GHz resonance frequencies.

and the calculated value of third resonance frequency $f_{r3} = 5.87$ GHz. Therefore, it may be concluded that calculated values of first, second and third resonance frequencies are much close to simulated values. The fourth wide operating band is achieved due to basic offset CPW-fed monopole antenna structure.

2.5. Parametric study

In order to see an impact of different parameters of the proposed antenna on multiband and CP behavior, the parametric studies of $|S_{11}|$ and AR for different values of W_6, W_3, W_1, t_1 and s_1 have been presented. In these variations, one parameter is varied at a time and keeping other parameters constant to analyze the impact on reflection coefficient and AR.

2.5.1. The effect of tilted length W_6

The effect of tilted length W_6 in $|S_{11}|$ and AR on antenna performance is depicted in Fig. 7(a) and (b), respectively. As can be seen from Fig. 7(a), the tilted length W_6 affects only the first resonance frequency while it has no effect on other resonance frequencies and operating bands. As tilted length increased then first resonance frequency is shifted towards lower side while the first AR band tends to disappear and higher AR bands unchanged as shown in Fig. 7(b). It means that the tilted length W_6 has impact on first resonance and first AR band because the rectangular slot on upper arm of tilted E-shaped monopole help to improve first AR band. So, we can tune tilted length W_6 to obtain the required IBWs and ARBWs. Based on the study, we choose $W_6 = 25.46$ mm.

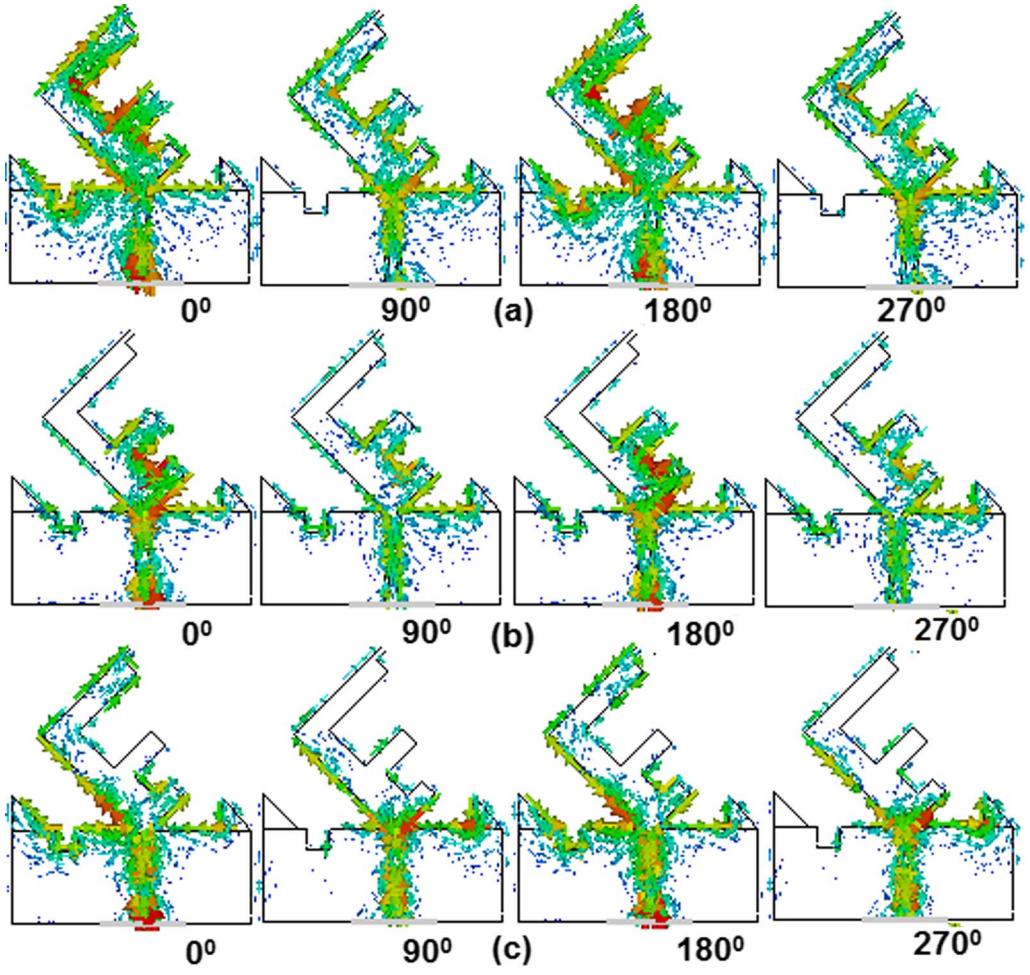

Fig. 6. Surface current distribution of the proposed tilted asymmetrical E-shaped printed antenna at (a) 3.3 GHz, (b) 5.05 GHz, and (c) 7.3 GHz CP frequencies.

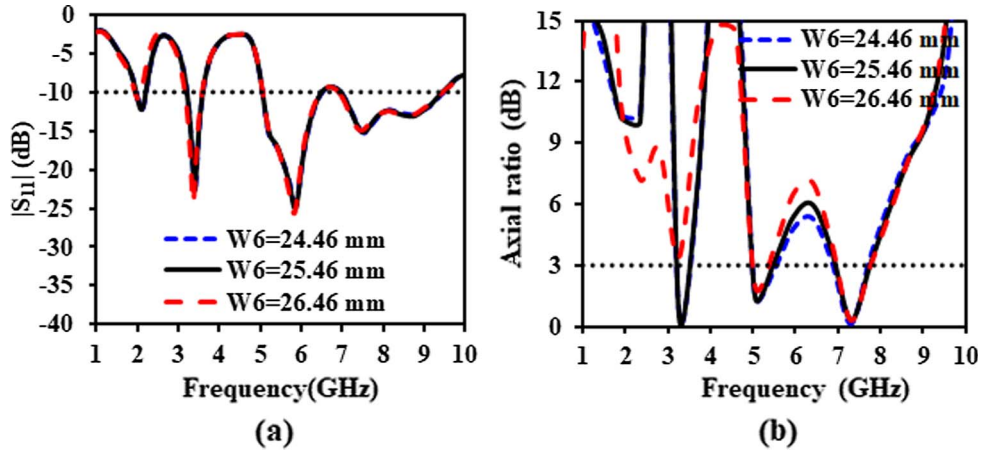

Fig. 7. Effect of tilted length W_6 on antenna performance: (a) $|S_{11}|$, (b) AR.

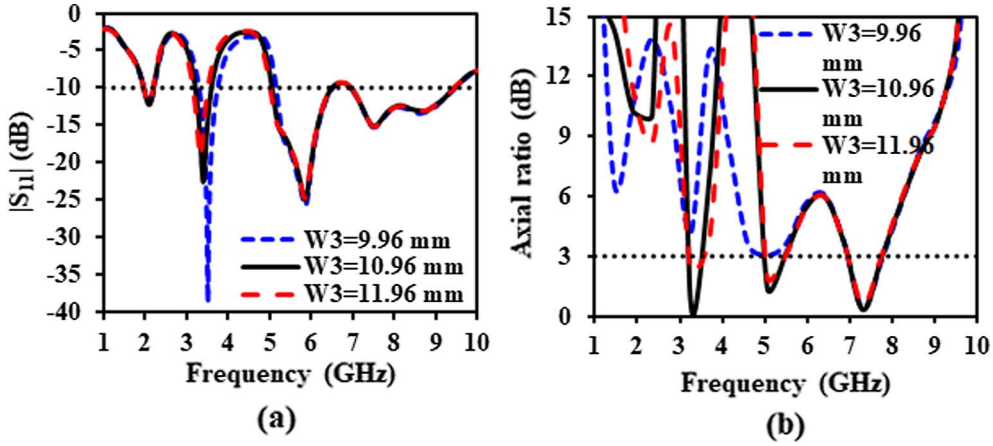

Fig. 8. Effect of tilted length W_3 on antenna performance: (a) $|S_{11}|$, (b) AR.

2.5.2. The effect of tilted length W_3

The effect of tilted length W_3 in $|S_{11}|$ and AR on antenna performance is depicted in Fig. 8(a) and (b), respectively. As can be seen from Fig. 8(a), the tilted length W_3 affects only the second resonance frequency while it has no effect on other resonance frequencies and operating bands. As tilted length increased then second resonance frequency is shifted towards lower side. At $W_3 = 9.96$ mm, the first and second AR bands tends to disappear while at $W_3 = 11.96$ mm, the first band AR becomes poor and higher AR bands unchanged as shown in Fig. 8(b). It means that the tilted length W_3 has impact on second resonance and AR bands. So, we can tune tilted length W_3 to obtain the required IBWs and ARBWs. Based on the study, we choose $W_3 = 10.96$ mm.

2.5.3. The effect of tilted length W_1

The effect of tilted length W_1 in $|S_{11}|$ and AR on antenna performance is depicted in Fig. 9(a) and (b), respectively. As can be seen from Fig. 9(a), the tilted length W_1 affects the lower edge frequency of third band and upper edge frequency of fourth band while it has no effect on first and second resonance frequencies and operating bands. As tilted length increased then lower/upper edge frequencies of third/fourth band are shifted towards lower side, respectively. In addition, when W_1 increased then only second AR band is affected as shown in Fig. 9(b). At $W_1 = 11.58$ mm, the second band AR becomes poor and other AR bands are unchanged. It means that the tilted length W_1 has impact on $|S_{11}|$ in mainly third band and second AR band. So, we can tune tilted length W_1 to obtain the required IBWs and ARBWs. Based on the study, we choose $W_1 = 10.58$ mm.

2.5.4. The effect of length t_1 of triangular stub

The effect of length t_1 of triangular stub on antenna AR is depicted in Fig. 10(a). As can be seen from Fig. 10(a), the length t_1 affects the second and third AR bands while it has no effect on first AR band. At $t_1 = 5$ mm, the second and third band has poor AR and touches 3-dB ARBW line. At $t_1 = 6$ mm, the second and third band AR is slightly improved. Similarly, at $t_1 = 8$ mm and 9 mm, the second band AR becomes poor and second AR band goes to disappear. It means that the length t_1 has impact on second and third AR bands. So, we can tune length t_1 to obtain the required ARBWs in second and third bands. Based on the study, we choose $t_1 = 7$ mm.

2.5.5. The effect of rectangular slot length s_1

The effect of rectangular slot length s_1 on antenna AR is depicted in Fig. 10(b). As can be seen from Fig. 10(b), the slot length s_1 affects the all three AR bands. At $s_1 = 2$ mm, the first and second band has poor AR and goes to disappear while third AR band has a small ARBW. At $s_1 = 3$ mm, the all bands AR is slightly improved. Further, to increase slot length $s_1 = 4$ mm then AR is improved and all desired bands are obtained. At $s_1 = 5$ mm, the second and third AR bands are closed spaced formed a single AR band and provide wide ARBW. At $s_1 = 6$ mm, the first AR band goes to disappear and ARBW is decreased as s_1 increased from 5 mm to 6 mm. It means that the slot length s_1 has impact on all three AR bands. So, we can tune length s_1 to obtain the required ARBWs. Based on the study, we choose $s_1 = 4$ mm. For CP radiation, the magnitude of electric field components is identical ($Ex = Ey$) and 90° phase difference (PD) between them. For $s_1 = 4$ mm and $t_1 = 7$ mm, the $|Ex/Ey|$ ratio and PD plot is shown in Fig. 10(c) and

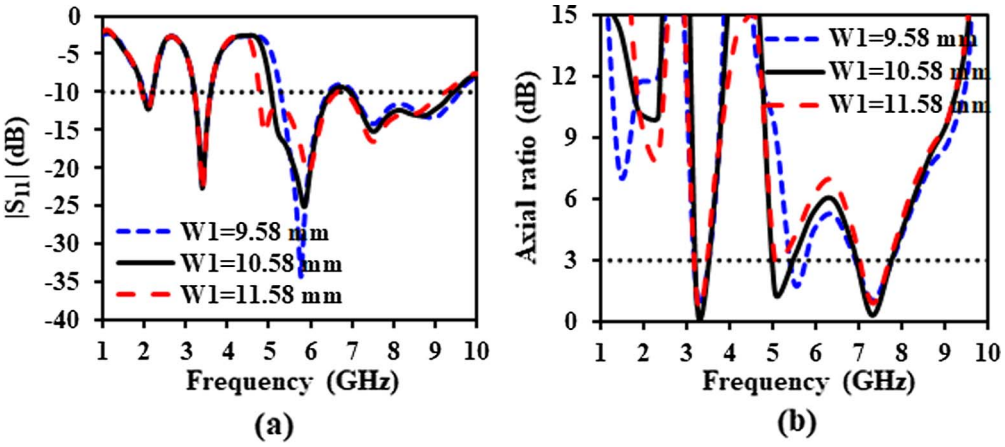

Fig. 9. Effect of tilted length W_1 on antenna performance: (a) $|S_{11}|$, (b) AR.

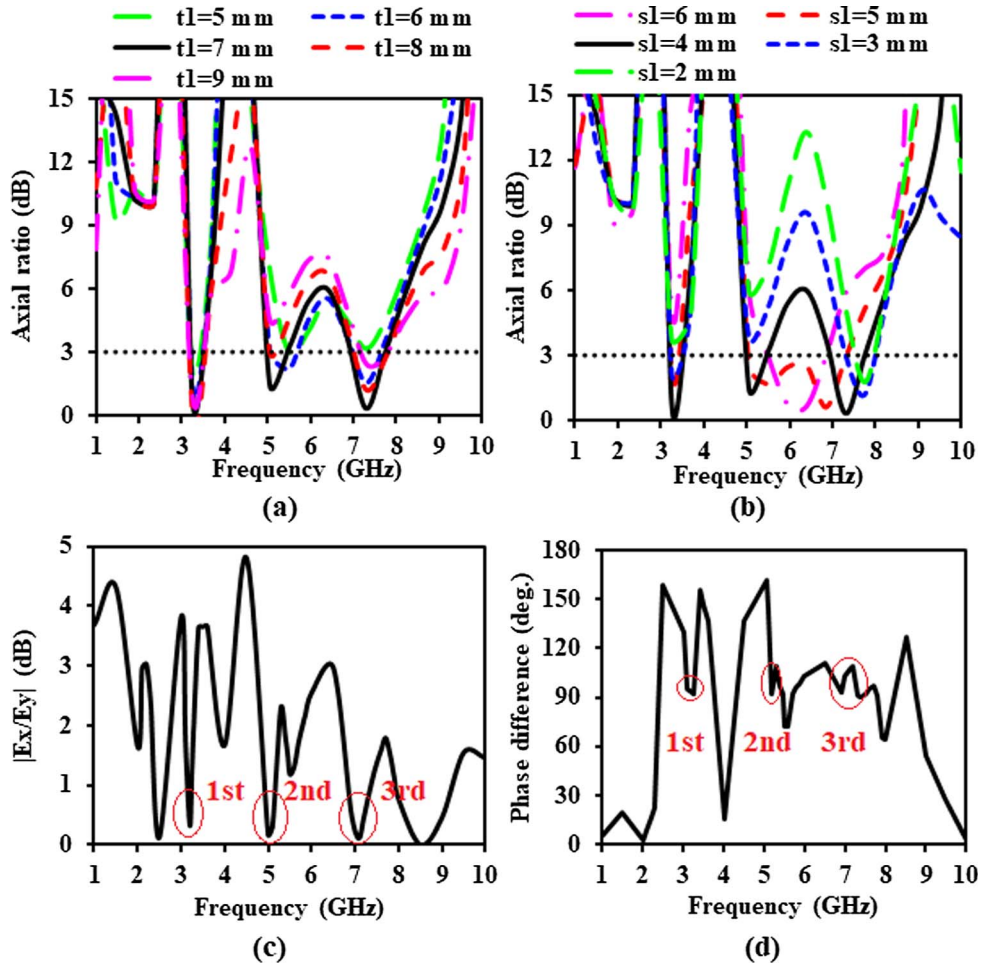

Fig. 10. Antenna axial ratio (a) effect of t_1, (b) effect of s_1; for s_1 = 4 mm and t_1 = 7 mm, simulated (c) amplitude ratio, and (d) phase difference.

(d), respectively. It can be seen from oval regions of Fig. 10(c) and (d) that at first, second and third CP band, the two electric fields components with almost identical amplitudes and 90^0 PD is introduced. As a result, the antenna shows triple CP waves and provides triple CP bands. In the first 2.1 GHz operating band, the unequal amplitudes with 0° PD is observed so that antenna generates linearly polarized wave.

3. Experimental results and discussion

To validate the proposed offset CPW-fed tilted asymmetrical E-shaped printed antenna, the antenna is fabricated using MITS eleven lab and photograph of prototype antenna is depicted in Fig. 11(a). Fig. 11(b) shows the measurement setup used for radiation characteristics of the proposed antenna in anechoic chamber. $|S_{11}|$ is measured with Agilent PNA-N5234A network analyzer to verify the performance of the antenna. The simulated and measured $|S_{11}|$ and ARs curves are plotted in Figs. 12 and 13, respectively. As can be observed from Fig. 12, the measured −10 dB IBWs are 220 MHz (2.04–2.26 GHz), 580 MHz (3.22–3.80 GHz), 1570 MHz (5.08–6.65 GHz), and 2840 MHz (7.10–9.94 GHz). The measured 3-dB ARBWs are 230 MHz

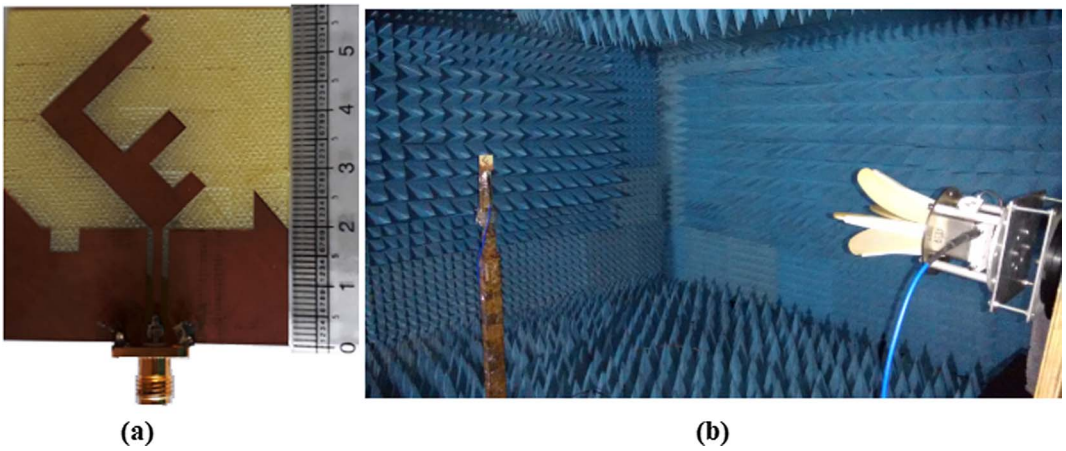

Fig. 11. (a) Fabricated prototype, (b) measurement setup of the proposed antenna.

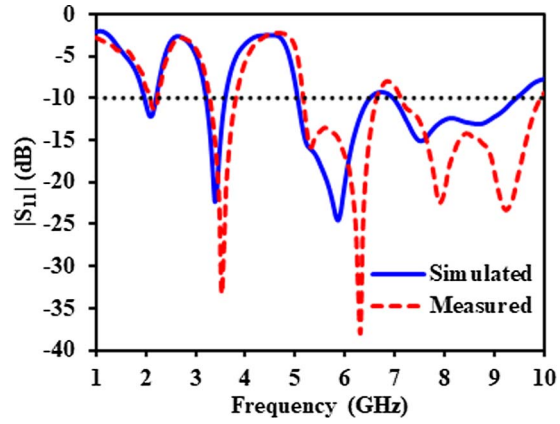

Fig. 12. Simulated and measured $|S_{11}|$ of the proposed antenna.

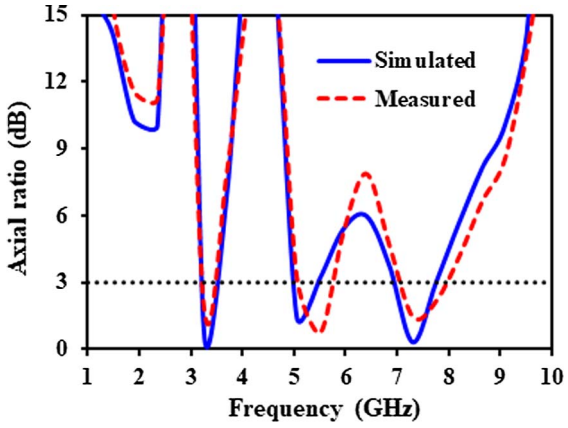

Fig. 13. Simulated and measured AR of the proposed antenna.

(3.25–3.48 GHz), 710 MHz (5.12–5.83 GHz), and 880 MHz (7.15–8.03 GHz) achieved at theta = 0° and phi = 0° as shown in Fig. 13. The slight shift observed in simulated and measured resonance frequencies and bands which can be credited to dissimilarity in dielectric material properties of commercial available and considered material for simulation, not using Sub-Miniaturized Type-A (SMA) connector in simulation, residuals of soldering metal pieces on CPW ground plane, fabrication and measurement errors. Fig. 14(a)–(d) displays the simulated and measured radiation patterns at frequencies 2.1 GHz, 3.3 GHz, 5.3 GHz, and 7.5 GHz in the *xz*-plane (phi = 0°) and *yz*-plane (phi = 90°), respectively. The radiation pattern measurement is carried out in anechoic chamber using LB-OSJ-20,180-P03 dual

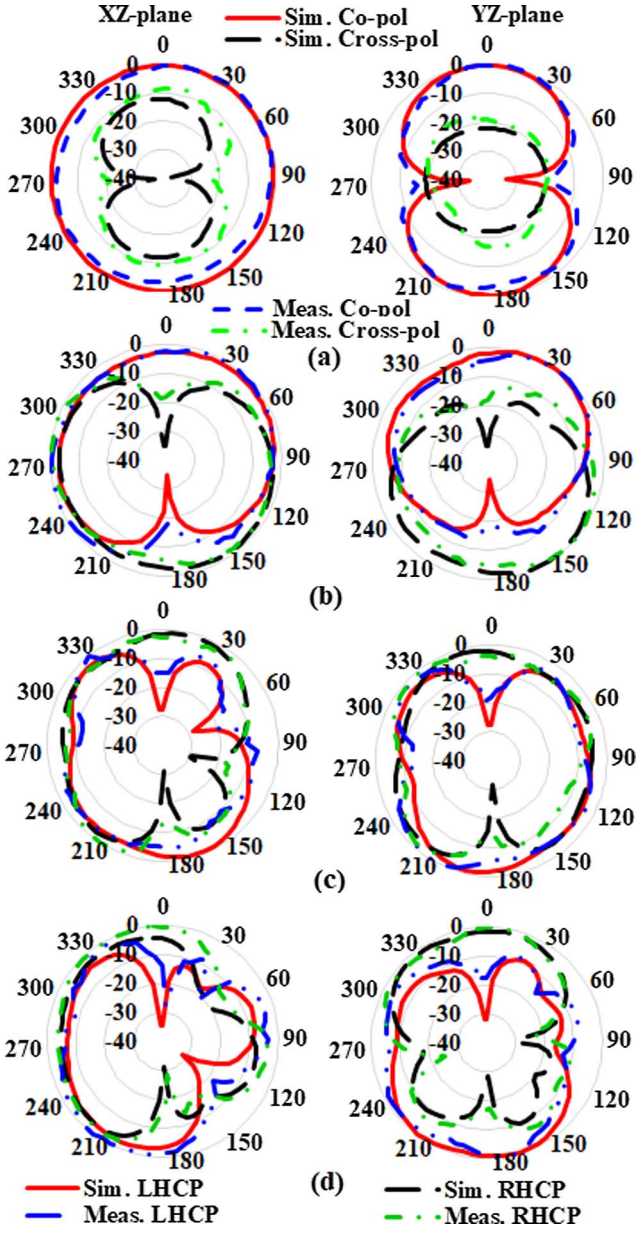

Fig. 14. Radiation patterns of the proposed tilted asymmetrical E-shaped printed antenna at (a) 2.1 GHz, (b) 3.3 GHz, (c) 5.3, and (c) 7.5 GHz.

Table 3
The range of angles around broadside direction where AR ≤ 3-dB.

Frequency (GHz)	3.3	5.3	7.5
xz-plane	$\theta = 45^{\circ}$	$\theta = 15^{\circ}$	$\theta = -40^{\circ}$
yz-plane	$\theta = 30^{\circ}$	$\theta = -15^{\circ}$	$\theta = 15^{\circ}$
Polarization	LHCP	RHCP	RHCP

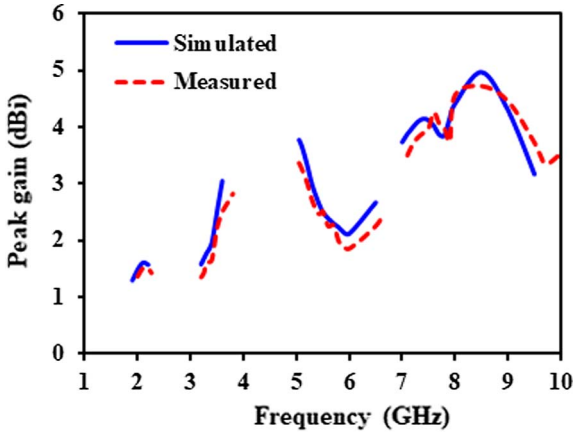

Fig. 15. Simulated and measured peak gain of the proposed antenna.

circular polarized horn antenna as reference antenna and proposed antenna placed on rotator table considered as antenna under test (AUT) as shown in Fig. 11(b). As can be seen from Fig. 14(a) that the co-polarized radiation pattern at 2.1 GHz frequency is omnidirectional in *xz*-plane and bi-directional in *yz*-plane. At 2.1 GHz, the co- and cross-polarization difference in the boresight direction is ~18 dBi in *yz*-plane and ~10 dB in *xz*-plane. As a result, it provides linear polarization radiation in both planes. As can be seen from Fig. 14(b) that the radiation pattern at 3.3 GHz CP frequency, the antenna radiates LHCP wave in the $+z$ direction whereas RHCP wave in the $-z$ direction in *xz*-plane and *yz*-plane. In both planes, the cross polarization level is measured to be > 17 dB at theta = 0° which shows good CP radiation. As can be seen from Fig. 14(c) and (d) that the radiation pattern at 5.3 GHz and 7.5 GHz CP frequencies, the antenna radiates RHCP wave in the $+z$ direction and LHCP wave in the $-z$ direction in *xz*-plane and *yz*-plane but slightly tilted from main axis due to asymmetrical geometry of tilted E-shaped monopole antenna. In both planes at 5.3 GHz and 7.5 GHz, the cross polarization level is measured to be > 15 dB at theta = 0° which shows good CP radiation. From the results, it can be seen that the good agreement obtained between simulated and measured radiation patterns. Moreover, in broadside direction the range of angles over which AR ≤ 3-dB is specified in Table 3 at three CP frequencies.The simulated and measured peak gain against frequency is plotted in Fig. 15. It is observed that the antenna shows measured gain variation in first band 1.36–1.52 dBi while simulated gain variation 1.30–1.63 dBi. In second band, the measured antenna LHCP gain varies 1.35–2.83 dBi while simulated LHCP gain varies 1.59–3.05 dBi. The measured antenna RHCP gains varies in third/fourth band is 1.86–3.37/3.50–4.74 dBi while the simulated RHCP gains 2.12–3.78/3.73–4.97 dBi in the broadside direction, respectively. As a result, good agreement between simulated and measured peak gains is observed. Table 4 summarizes the performance comparison of proposed work with some other previously published dual/triple band circularly polarized antennas. The proposed antenna has advantages of wide quad-band functionality, triple-band circular polarization features, simple structure, easy design procedure and good LP/LHCP/RHCP radiations as compared to previous researchers of single/dual/triple operating bands along with dual/triple-band CP band antennas [12–19].

4. Conclusions

An offset CPW-fed triple-band circularly polarized tilted asymmetrical E-shaped printed antenna for multiband wireless applications is presented. With the proper offset in feed, embedding of two triangular stubs and small rectangular slot in modified CPW ground plane along

Table 4
Comparison of proposed work with previously published dual/triple CP antennas.

Ref.	Size (mm^2)	IBW (GHz, f_c, %)	$\|S_{11}\| < -10$ dB bands	3-dB ARBWs (GHz, f_{cp}, %)	3-dB ARBW bands	Polarization
[12]	55 × 66	1.527–1.917, 1.722, 22.7 2.598–3.248, 2.923, 22.3	Dual	1.579–1.637, 1.61, 3.6 2.67–2.822, 2.74, 5.6	Dual	LHCP RHCP
[13]	40 × 39	2.17–8.47, 5.32, 118.4	Single	2.41–2.55, 2.48, 5.6 3.45–4.35, 3.9, 23.1	Dual	LHCP RHCP
[14]	70 × 70	1.4–4.0, 2.7, 96.29	Single	1.48–1.75, 1.62, 16.72 3.4–3.57, 3.48, 4.7	Dual	RHCP LHCP
[15]	40 × 40	2.446–2.558, 2.502, 4.47 3.466–3.584, 3.525, 3.34 5.635–6.062, 5.84, 7.3	Triple	2.482–2.497, 2.49, 0.6 3.54–3.584, 3.57, 1.23 5.708–5.744, 5.72, 0.62	Triple	RHCP RHCP RHCP
[16]	55 × 52	2.35–2.8, 2.575, 17.47 3.3–7.4, 5.35, 76.63	Dual	2.35–2.65, 2.45, 12 3.3–3.65, 3.5, 10 5.6–5.85, 5.8, 4.4	Triple	LHCP LHCP LHCP
[17]	60 × 60	3.22–4.5, 3.88, 33.16 4.76–5.98, 5.37, 22.72	Dual	3.49–3.55, 3.52, 1.7 4.06–4.22, 4.14, 3.86 5.03–5.3, 5.16, 5.23	Triple	RHCP RHCP RHCP
[18]	44 × 46	2.37–7.89, 5.13, 107.6	Single	2.22–2.83, 2.45, 24.2 2.92–3.79, 3.5, 25.9 5.45–5.98, 5.8, 9.3	Triple	LHCP LHCP LHCP
[19]	65 × 45	1.57–1.85, 1.71, 16.37 1.99–2.19, 2.09, 9.56 2.52–2.77, 2.645, 9.45	Triple	1.56–1.62, 1.57, 3.70 1.98–2.08, 2.02, 4.90 2.50–2.63, 2.55, 5.06	Triple	RHCP LHCP LHCP
Our work	50 × 58	2.04–2.26, 2.15, 10.23 3.22–3.80, 3.51, 16.52 5.08–6.65, 5.865, 26.76 7.10–9.94, 8.52, 33.33	Quad	– 3.25–3.48, 3.36, 6.84 5.12–5.83, 5.47, 12.97 7.15–8.03, 7.59, 11.59	Triple	LP LHCP RHCP RHCP

with rectangular slot in the longer arm of tilted asymmetrical E-shaped radiator, the triple-band circular polarization has been achieved. The measured antenna has 3-dB ARBWs of 230 MHz (3.25–3.48 GHz), 710 MHz (5.12–5.83 GHz), and 880 MHz (7.15–8.03 GHz) whereas −10 dB IBWs of 220 MHz (2.04–2.26 GHz), 580 MHz (3.22–3.80 GHz), 1570 MHz (5.08–6.65 GHz), and 2840 MHz (7.10–9.94 GHz). Wide quad-band functionality, triple circular polarization bands, simple structure with good LHCP/RHCP radiations makes the proposed antenna is a good candidate of various wireless applications such as UMTS-2100, 3.5/5.5 GHz WiMAX, 5.2/5.8 GHz WLAN, ITS, downlink of X-band satellite communication, and ITU 8 GHz.

Acknowledgements

The authors would like to acknowledge and convey their sincere thanks to Prof. Kumar Vaibhav Srivastava, of Indian Institute of Technology (IIT), Kanpur, Uttar Pradesh, India and Government Mahila Engineering College, Ajmer, India for providing necessary facilities of measurement lab to complete this research work.

References

[1] Ghobadi A, Dehmollaian M. A printed circularly polarized Y-shaped monopole antenna. IEEE Anten Wireless Propag Lett 2012;11:22–5.
[2] Kushwaha N, Kumar R. Compact coplanar waveguide-fed wideband circular polarised antenna for navigation and wireless applications. IET Microw Anten Propag 2015;9(14):1533–9.
[3] Tang H, Wang K, Wu R, Yu C, Zhang J, Wang X. A novel broadband circularly polarized monopole antenna based on C-shaped radiator. IEEE Anten Wireless Propag Lett 2016;16:964–7.
[4] Ram Krishna RVS, Kumar R. Design of ultra-wideband trapezoidal shape slot antenna with circular polarization. Int J Electron Commun 2013;67(12):1038–47.
[5] Chen Q, Zhang H, Yang L-C, Min X-L. Wideband asymmetric microstrip-fed circularly polarized antenna with monofilar spiral stub for WLAN application. Int J RF Microw Comput Aided Eng 2017;27(8):e21128.
[6] Chen Z-F, Xu B, Hu J, He S. A CPW-fed broadband circularly polarized wide slot antenna with modified shape of slot and modifying feeding structure. Microw Opt Technol Lett 2016;58(6):1453–7.
[7] Goswami SA, Karia D. A compact monopole antenna for wireless applications with enhanced bandwidth. Int J Electron Commun 2017;72:33–9.
[8] Kumar A, Jhanwar D, Sharma MM. A compact printed multistubs loaded resonator rectangular monopole antenna design for multiband wireless systems. Int J RF Microw Comput Aided Eng 2017;27(9):e21147.
[9] Saxena S, Kanaujia BK, Dwari S, Kumar S, Tiwari R. A compact microstrip fed dual polarized multiband antenna for IEEE 802.11a/b/g/n/ac/ax applications. Int J Electron Commun 2017;72:95–103.
[10] Kumar A, Deegwal JK, Sharma MM. Design of multi-polarised quad-band planar antenna with parasitic multistubs for multiband wireless communication. IET Microw Anten Propag 2017. http://dx.doi.org/10.1049/iet-map.2017.0526.
[11] Khandelwal MK, Kanaujia BK, Deari S, Kumar S, Gautam AK. Triple band circularly polarized compact microstrip antenna with defected ground structure for wireless applications. Int J Microw Wireless Technol 2016;8(6):943–53.
[12] Wang C, Li J, Zhang A, Joines WT, Liu QH. Dual-band capacitively loaded annular-ring slot antenna for dual-sense circular polarization. J Electromagn Waves Appl 2017;31(9):867–78.
[13] Jou CF, Wu J-W, Wang C-J. Novel broadband monopole antennas with dual-band circular polarization. IEEE Trans Anten Propag 2009;57(4):1027–34.
[14] Saini RK, Dwari S. Dual-band dual-sense circularly polarized square slot antenna with changeable polarization. Microw Opt Technol Lett 2017;59(4):902–7.
[15] Bao XL, Ammann MJ. Printed triple-band circularly polarised antenna for wireless systems. Electron Lett 2014;50(23):1664–5.
[16] Hoang TV, Park HC. Very simple 2.45/3.5/5.8 GHz triple-band circularly polarized printed monopole antenna with bandwidth enhancement. Electron Lett 2014;50(24):1792–3.
[17] Baek JG, Hwang KC. Triple-band unidirectional circularly polarized hexagonal slot antenna with multiple L-shaped slits. IEEE Trans Anten Propag 2013;61(9):4831–5.
[18] Tang H, Wang K, Wu R. Compact triple-band circularly polarized monopole antenna for WLAN and WiMAX applications. Microw Opt Technol Lett 2017;59(8):1901–8.
[19] Brar RS, Saurav K, Sarkar D, Srivastava KV. A triple band circular polarized monopole antenna for GNSS/UMTS/LTE. Microw Opt Technol Lett 2017;59(2):298–304.